Ma et al. *Zool. Res. Divers. Conserv.* 2024, 1(4): 262−272
https://doi.org/10.24272/j.issn.2097-3772.2024.008
https://cstr.cn/32249.14.zrdc.2024.008

ZRDC Zoological Research: Diversity and Conservation

Article Open Access

Evolutionary history of multiple mountain ungulates reveals refugia and population expansion in response to Quaternary change in the East Himalaya-Hengduan Mountains

Xiao-Ying Ma[1,3], Nan Sun[1,4], Yun Fang[2], Zeng-Ping Yang[1,3], Ye Htet Lwin[2,6,7], Guo-Gang Li[1,3,5,*]

[1] *College of Life Sciences*, *Qinghai Normal University*, *Xining*, *Qinghai* 810008, *China*

[2] *Center for Integrative Conservation*, *Xishuangbanna Tropical Botanical Garden*, *Chinese Academy of Sciences*, *Mengla*, *Yunnan* 666303, *China*

[3] *Academy of Plateau Science and Sustainability*, *Qinghai Normal University*, *Xining*, *Qinghai* 810016, *China*

[4] *School of Life Sciences*, *Zhengzhou University*, *Zhengzhou*, *Henan* 450001, *China*

[5] *Key Laboratory of Biodiversity Formation Mechanism and Comprehensive Utilization of the Qinghai-Xizang Plateau in Qinghai Province*, *Qinghai Normal University*, *Xining*, *Qinghai* 810008, *China*

[6] *Southeast Asia Biodiversity Research Institute*, *Chinese Academy of Sciences*, *Yezin*, *Nay Pyi Taw* 05282, *Myanmar*

[7] *Wildlife Ecology and Conservation Biology*, *Faculty of Environment and Natural Resources*, *University of Freiburg*, *Freiburg* 79085, *Germany*

ABSTRACT

Quaternary geological events, glacial cycles, and climate fluctuations have a profound influence on the evolutionary history and population dynamics of many species. Mountain ungulates offer an ideal model for researching these historical processes. In this study, three taxa of mountain ungulates (*Capricornis*, *Naemorhedus*, and *Muntiacus*), which share overlapping ecological niches and similar life-history strategies, were selected to analyze the impact of historical events on their evolution and population dynamics. Specimens were collected from naturally deceased individuals during multiple field expeditions, as well as from forest police seizures, and included skulls, skins, and dried meat. Mitochondrial genomes (mitogenomes) were used as molecular markers. Analyses indicated that the evolutionary divergence of these mountain ungulates was primarily driven by five major uplift phases of the Qinghai-Xizang Plateau and a series of glaciation events. Results also indicated the formation of multiple refugia in the East Himalaya-Hengduan Mountains (EHHM) during the Quaternary. Four species—*C. sumatraensis*, *N. cranbrooki*, *N. evansi*, and *M. gongshanensis*—were selected for detailed analyses of historical population dynamics. Notably, population expansions were detected for all species, with the expansions of *N. cranbrooki*, *N. evansi*, and *M. gongshanensis* occurring during the early to mid-Holocene, likely due to warmer and more humid climatic conditions. In contrast, the population expansion of *C. sumatraensis* occurred in the late Holocene, driven by forest retreat and increased human activities such as settlement and grazing. Additionally, and most importantly, we obtained molecular samples of *N. cranbrooki* in Xizang, China, for the first time, and also confirmed the distribution of *N. cranbrooki* in Xizang rather than being limited to northern Myanmar. Overall, these findings provide evidence that *N. cranbrooki* is distributed in Xizang, also offer novel insights into the connections between Quaternary environmental change and species differentiation, refugia formation and population dynamics of mountain ungulates in the EHHM region.

Keywords: Mitogenomes; Glacier; Refugia; Population expansion; Quaternary change

INTRODUCTION

The Quaternary represents one of the most significant periods of climatic change in Earth's history, characterized by repeated glacial advances and retreats (Barnosky, 2005).

Received: 17 May 2024; Accepted: 27 August 2024; Online: 30 August 2024

Foundation items: This work was supported by the National Natural Science Foundation of China (32360133, 31901080), Transboundary Cooperation on Biodiversity Research and Conservation in Gaoligong Mountains (No. E1ZK251) and Major Science and Technique Programs in Yunnan Province (Grant No. 202102AA310055)

*Corresponding author, E-mail: liguogang@xtbg.ac.cn

These climatic shifts were largely driven by the periodic uplift of the Qinghai-Xizang Plateau, caused by regular changes in the Earth's orbital parameters (Candy, 2023). The Quaternary is divided into two epochs: The Pleistocene, spanning approximately 2.6 million years ago (Ma) to 11 700 years ago (Barnosky, 2005; Schaefer et al., 2016) and the Holocene, beginning approximately 11 700 years ago and continuing to present day (Gibbard, 2015; Head & Gibbard, 2015).

During the late Mesozoic and Quaternary periods, the Qinghai-Xizang Plateau underwent multiple uplift phases and experienced complex climatic transformations. The Pleistocene, in particular, was shaped by these repeated uplift events and the formation of extensive ice sheets, ice caps, and valley glaciers. According to the record, in addition to the Qinghai-Xizang Plateau and its adjacent region experienced tectonic rotation and strike-slip motion with minor uplift around 8 Ma (Zhang et al., 2006), it also underwent five major uplift phases, including the A phase (3.6 Ma), B phase (2.6 Ma), and C phase (1.7–1.66 Ma) of the Qinghai-Xizang Movement, followed by the Kunlun-Huanghe Movement (1.1–0.7 Ma) and Gonghe Movement (0.15 Ma) (Cui et al., 2011; Li et al., 2015). During the A phase of the Qinghai-Xizang Movement (3.6 Ma), the entire Qinghai-Xizang Plateau was elevated, leading to the disintegration of the primary planation plane (Raymo & Ruddiman, 1992). This uplift coincided with a critical period of global cooling, resulting in widespread glacier formation, although Asia remained largely unaffected due to insufficient mountain elevation for glacier development (Cui et al., 2011). During the B phase of the Qinghai-Xizang Movement (2.6 Ma), the plateau further uplifted to a critical height of 2 000 m, triggering the development of the Asian monsoon system (Li et al., 2001), aridification of the Asian interior, and cooling of the northern hemisphere (Cai et al., 2012; Zachos et al., 2001). During the C phase of the Qinghai-Xizang Movement, several Himalayan peaks surpassed 4 000 m in height, combined with the climate of the ice age at that time, the earliest Shishapangma ice age occurred (Zheng & Shi, 1976). The Kunlun-Huanghe Movement (1.1–0.7 Ma) further elevated the plateau beyond 3 000 m, creating conditions favorable for widespread glaciation. Glaciers expanded southward to the Himalayas, northward to the Kunlun and Tianshan mountains, eastward to the Hengduan Mountains, and westward to the Karakoram Mountains, marking the onset of the glaciation period across the region (Cui et al., 1998). Geological changes, such as mountain uplift, fragmented habitats and created barriers to gene flow, accelerating the genetic differentiation of local species (Antonelli et al., 2009; Xu et al., 2010). Fossil and moraine records indicate that the Qinghai-Xizang Plateau and surrounding regions experienced multiple Pleistocene glaciations during Pleistocene periods (Shi et al., 1992; Shi, 2002), including the Xixiabangma (1.17–0.8 Ma), Naynayxungla (0.7–0.5 Ma), Guxiang (0.3–0.13 Ma), and Baiyu (0.07–0.01 Ma) glaciations (Zheng et al., 2002).

In response to these spatiotemporal fluctuations in environmental conditions, refugia—areas that provide stable conditions for species survival—played critical roles in species persistence (Hewitt, 2000; Schmitt & Varga, 2012; Stewart et al., 2010). These refugia offered survival geographical opportunities for retreated species during adverse climatic periods, then they recolonizated during more favorable conditions (Morales-Barbero et al., 2018). Mountains, in particular, served as important refugia due to their high habitat heterogeneity, complex topography, climatic diversity, and low human disturbance (Zu & Wang, 2022). Fossil evidence from Mainland of China suggests that early Pliocene fauna adapted to warm, wet conditions retreated southeastward during glacial periods when northern regions became much cooler and drier (Li et al., 2004). Temporary mountain glaciers acted as physical barriers, isolating populations in refugia and promoting population differentiation and intraspecific diversification (Hewitt, 2000; Meng et al., 2015). Consequently, refugia tend to exhibit high species diversity (Gómez & Lunt, 2007; Whittington-Jones et al., 2008; Willner et al., 2009) and a high proportion of endemic species (Fjeldsaå & Lovett, 1997).

The Holocene, in contrast, has been marked by more variable climatic changes, influenced by both natural and human factors. Climatic fluctuations during the Quaternary are recognized as key drivers of evolutionary succession, shaping genetic and geographic structures, and influencing demographic dynamics of across various regions (Domingo et al., 2013; Lorenzen et al., 2011; Mapelli et al., 2012). Indeed, many species experienced population contractions and expansions in response to cold-warm climatic oscillations throughout the Quaternary, which significantly impacted their diversity and distribution (Fu & Wen, 2023). Climate change remains a major determinant of vegetation distribution and abundance (Bartlein et al., 1986; Ma et al., 2013), which, in turn, governs the population dynamics of herbivores by determining food availability and energy resources.

The East Himalaya-Hengduan Mountains (EHHM) region, a key extension of the Qinghai-Xizang Plateau, is one of the most well-known biodiversity hotspots in the world (Myers et al., 2000). This region not only serves as a center for the diversification and origin of many taxa (Hu, 1994; Jia et al., 2012) but is also considered as a critical glacial refuge for many species during the Quaternary glaciations (Frenzel et al., 2003; Wu, 1988; Yang et al., 2008). The EHHM harbors a rich diversity of mammals, including a notable number of endemic and rare species, such as *Muntiacus vaginalis*, *M. gongshanensis*, *M. putaoensis*, *Naemorhedus cranbrooki*, *N. evansi*, *N. baileyi*, *Capricornis rubidus*, *C. sumatraensis* (Li et al., 2017; Lwin et al., 2021; Zhang et al., 2021b), *Macaca munzala* (Sinha et al., 2005), and *Rhinopithecus strykeri* (Geissmann et al., 2011; Yang et al., 2022). Given the complex topography of the region, the EHHM likely contained many refugia during glacial cycles, providing critical habitats for species survival and fostering biodiversity through isolation and subsequent diversification.

Mountain ungulates provide an ideal model for investigating the impacts of geological and climate changes on population history and dynamics due to their adaptation to alpine environments, where they endure harsh and highly variable conditions (Willisch et al., 2013). This is particularly relevant in the EHHM region, which has a complex geological and climatic history. Among mountain ungulates, serows are of significant interest, with four species listed in the IUCN (International Union for Conservation of Nature) Red List, including Japanese serow (*C. crispus*), Formosan serow (*C. swinhoei*), Burmese red serow (*C. rubidus*), and mainland serow (*C. sumatraensis*). The classification of *C. sumatraensis* remains controversial, with ongoing debate about whether the Chinese serow (*C. milneedwardsii*), Himalayan serow (*C. thar*) and Sumatran serow (*C. sumatraensis*) should be considered a species or subspecies as mainland serow (*C. sumatraensis*) or three distinct species (Supplementary table S1). Gorals,

once classified within the same genus as serows, were reclassified into a separate genus in 1985 (Groves & Grubb, 1985). The IUCN Red List contains three goral species, including the long-tailed goral (*N. caudatus*), Himalayan goral (*N. goral*), and red goral (*N. baileyi*). However, whether *N. baileyi* and *N. cranbrooki* represent the same or different species remains an unresolved taxonomic issue (Supplementary table S2). Thirteen species of muntjacs are included in the IUCN Red List, with the main taxonomic dispute being whether *Muntiacus gongshanensis* and *M. crinifrons* are the same or different species (Supplementary table S3). Although *Capricornis*, *Naemorhedus*, and *Muntiacus* species share a common evolutionary history and similar life-history strategies, they differ in dispersal abilities and habitat preferences, which generally makes them more vulnerable to extinction compared to smaller mammals (Liow et al., 2008). At least three species or subspecies of each genus are found in the EHHM region. Among serows, *C. rubidus*, *C. thar*, *C. sumatraensis*, and *C. milneedwardsii* have been reported in the EHHM region (Dou et al., 2016; Lwin et al., 2021), and recent phylogenetic studies suggest the latter three should be classified as a single species —mainland serow (*C. sumatraensis*) (Mori et al., 2019). Similarly, four goral species have been reported in the EHHM region, including the Burmese goral (*N. evansi*) (Li et al., 2020), Cranbrook's goral (*N. cranbrooki*) (Hayman, 1961; Li et al., 2020), *N. baileyi* (Velho et al., 2012), and *N. goral* (Liu & Jiang, 2017). Four muntjac species have been reported in the EHHM, including *M. putaoensis* (Li et al., 2017; Lwin et al., 2021), *M. gongshanensis* (Timmins & Duckworth, 2016; Zhang et al., 2021b), *M. vaginalis* (Lwin et al., 2021), and *M. feae* (Zhang et al., 1984).

In this study, we obtained complete mitochondrial genome (mitogenome) sequences from five *C. sumatraensis* from northern Myanmar, 10 *N. cranbrooki* (four from Motuo in Xizang, six from northern Myanmar), four *N. evansi* (two from Gongshan and Deqin in Yunnan, two from northern Myanmar), and four *M. gongshanensis* (three from northern Myanmar and one from Yunnan). We also obtained a complete mitogenome of *N. baileyi* from a wild individual for the first time, as previous samples were exclusively from zoo specimens. Using these mitogenomes, we examined the drivers of intrageneric and intraspecific differentiation in *Capricornis*, *Naemorhedus*, and *Muntiacus* species, with a particular focus on identifying potential evolutionary refugia in the EHHM region. Additionally, we investigated the historical demographic responses of four species (*C. sumatraensis*, *N. cranbrooki*, *N. evansi*, and *M. gongshanensis*) to Quaternary climate fluctuations in the EHHM region. This study provides critical insights into the relationships among Quaternary geological events, glacial cycles, climate change, species differentiation, and refugia formation, while also informing the development of effective conservation strategies for preserving species diversity.

MATERIALS AND METHODS

Sample sources

Five *C. sumatraensis* specimens, ten *N. cranbrooki* specimens, four *N. evansi* specimens, four *M. gongshanensis* specimens, and one *N. baileyi* specimen were obtained from the EHHM region (Figure 1), including three legs, 11 skulls, eight skins, and two dried meats (Supplementary table S4). Samples were collected from ungulates that died naturally during multiple field expeditions and from specimens confiscated by forest police from hunters. All samples were initially identified based on morphological characters recorded in Groves & Grubb (2011). Only samples with a known locality were collected. All samples were dried and preserved in silica gel and deposited in the Southeast Asia Biodiversity Research Institute, Chinese Academy of Sciences, Myanmar Lab and the School of Life Sciences, Qinghai Normal University.

DNA extraction, polymerase chain reaction (PCR) amplification, and sequencing

All molecular work was performed in a separate facility under in a sterile environment to avoid cross-contamination. DNA was extracted using a DNeasy Blood & Tissue Kit (Qiagen, Germany), and its concentration and integrity were detected using 2% agarose gel electrophoresis. The volume of the master mixture for PCR was 50 μL, which contained 100 ng of template DNA, 1 μL (10 pmol) of each primer, 5.0 μL of 10×Taq buffer, 2 μL of dNTP (2.5 mmol/L), 2.0 U Taq DNA polymerase, and sterilized ultra-purified water. The PCR conditions were as follows: Predenaturation at 95℃ for 8 min, 35 cycles of denaturation at 95℃ for 45 s, annealing at 52℃–64℃ for 45 s, extension at 72℃ for 1 min, and final extension for 7 min at 72℃. Reactions were performed on a Veriti Thermal Cycler (Applied Biosystems, USA) and always included a negative control. An ABI PRISM 3700 Genetic Analyzer (Applied Biosystems, USA) was used to sequence both ends of the PCR products. The primers refer to Supplementary table S4 of Li et al. (2020).

Assembly and alignment

Chromas software (http://www.technelysium.com.au) was used to analyze the obtained sequences, and waveform diagrams were used to correct the sequences. DNA Star v.5.0 was used to splice genes after correction (Burland, 2000). The sorted sequences were aligned in GENEIOUS v.2019.1.1 using the default parameters of MAFFT v.7.245 (Rozewicki et al., 2019), and manually checked and corrected.

Phylogenetic relationships based on mitogenomes

In addition to the obtained sequences, we downloaded all available complete mitogenomes from the NCBI database (https://www.ncbi.nlm.nih.gov). In total, 20 serows and 26 gorals were used as the ingroup and one *Rupicapra rupicapra*, one *Oreamnos americanus*, and one *Pantholops hodgsonii* (Bibi, 2013; Hassanin et al., 2012) were used as the outgroup to analyze the phylogenetic relationships of *Capricornis* and *Naemorhedus* species (Supplementary table S5). Including the obtained and downloaded sequences, 20 complete *Muntiacus* mitogenomes were used as the ingroup and one *Elaphodus cephalophus*, one *Cervus elaphus*, and one *Hydropotes inermis* (Beller et al., 2006; Pang et al., 2008) were used as the outgroup (Supplementary table S5). All sequences were subjected to pairwise alignment in ClustalW (Higgins & Sharp, 1988). Maximum-likelihood (ML) and Bayesian inference (BI) phylogenetic trees were constructed using IQ-tree and MrBayes, respectively, in PhyloSuite v.1.2.2 (Zhang et al., 2020). The most appropriate nucleotide substitution models were selected using Akaike information criteria (AIC) in ModelFinder (Kalyaanamoorthy et al., 2017). The optimal models for serows and gorals were TIM2+F+R8 (IQ-tree) and GTR+F+I+G4 (MrBayes) and the optimal models for muntjacs were TIM2+F+R3 (IQ-tree) and GTR+F+I+G4

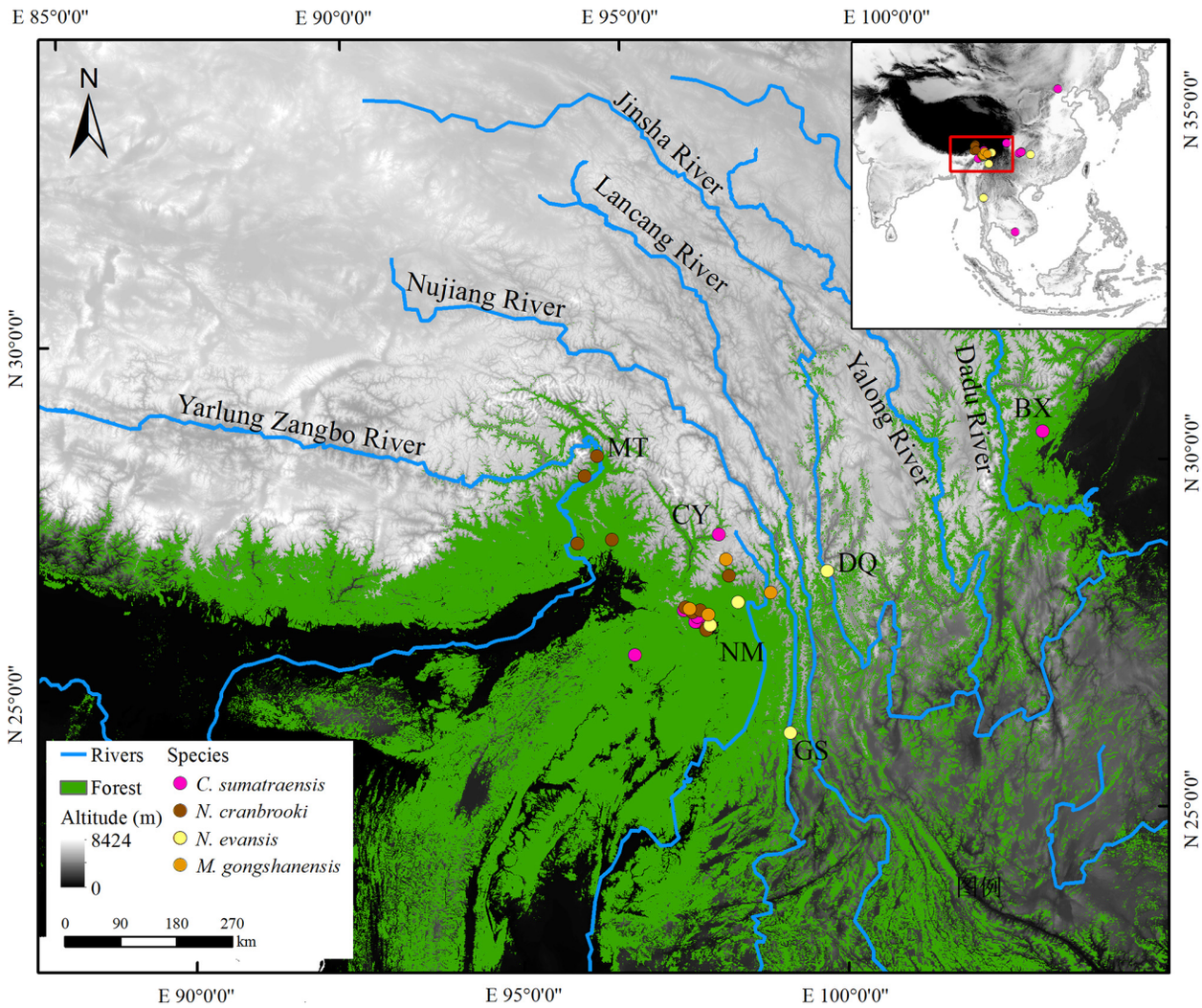

Figure 1 Geographic information on *Capricornis sumatraensis*, *Naemorhedus cranbrooki*, *Naemorhedus evansi*, and *Muntiacus gongshanensis* samples with known sampling locations

Samples included those obtained and those downloaded from the NCBI, with different species marked with different colored dots. Map in the upper right corner marks all species samples with known geographical locations. Red box marks East Himalaya-Hengduan Mountains region. MT and CY represent Motuo and Chayu in Xizang, China; GS and DQ represent Gongshan and Deqin in Yunnan, China; BX represents Baoxing in Sichuan, China; NM represents northern Myanmar.

(MrBayes). IQ-tree was run with 100 000 ultrafast bootstrap replicates. For Bayesian analysis, four Markov chain Monte Carlo (MCMC) chains were simultaneously run for 20 000 000 generations, with one tree randomly selected every 1 000 generations. Convergence diagnostics and discard values were assessed using Tracer v.1.7 (Rambaut et al., 2018), and the first 25% of samples were discarded as a conservative burn-in based on the diagnostic results. All trees were visualized using Figtree v.1.4.4 (http://tree.bio.ed.ac.uk/software/figtree).

Divergence times

Bayesian analysis was conducted using the same dataset as the phylogenetic relationships, employing MCMC implemented in BEAST v.2.7.5 (Bouckaert et al., 2014) with a Yule prior and strict molecular clock. The nucleotide substitution models were all GTR+F+G4, with empirical base frequencies, determined based on AIC in ModelFinder within PhyloSuite v.1.2.2. Three calibration points were used to estimate the divergence time of *Capricornis* and *Naemorhedus* species. Two of these calibration points, with age ranges and prior probability distributions, were derived from Bibi (2013): Internal calibration of the branching point between Caprini and Pantholops (95% highest posterior density interval (HPD)=9.3–11 Ma), and crown Caprini with a normal prior (mean=8.9 Ma, standard deviation=2 Ma) based on *Aragoral mudejar* (see Additional File 1 in Bibi, 2013). Another calibration point was based on the Sichuan (China) fossil record of *N. goral* from the Mid-Pleistocene (0.126 –0.781 Ma; Mead, 1989). Three calibration points were used to estimate the divergence time of *Muntiacus* species: The crown Cervidae (12.4–9.0 Ma) given in Bibi (2013), the split between Cervini and Muntiacini at 9±1 Ma based on fossils from the Late Miocene of China (Dong, 2007; Petronio et al., 2007), and the split between the red and black muntjacs (*M. crinifrons*), estimated at around 3.29 Ma (95% HPD=3.36–5.88; Singh et al., 2021). Three independent MCMC runs were performed, with sampling every 1 000 generations for 100 000 000 generations. A burn-in of 20% was applied, and the convergence of all parameters was assessed using Tracer v.1.7. The maximum clade credibility criterion tree was obtained using TreeAnnotator and visualized

with Figtree v.1.4.4.

Demographic history

The Extended Bayesian Skyline Plot (EBSP) was used to infer the historical population dynamics (Miller et al., 2018). EBSP analyses were implemented using the BEAST v.2.7.5 package. Complete mitogenomes of four species from the EHHM region (*C. sumatraensis*, *N. cranbrooki*, *N. evansi*, and *M. gongshanensis*) were selected for EBSP analysis with a strict molecular clock. The nucleotide substitution models were determined based on Bayesian Information Criterion (BIC) in ModelFinder within PhyloSuite v.1.2.2. The optimal model was HKY+F for all four species. The "Coalescent Extended Bayesian Skyline" model was used, with the "Population Model" factor set to 0.5 to account for female contribution to *Ne* (Heled & Drummond, 2008). Each population was run for 10 000 000 generations, with sampling every 1 000 steps and the first 10% of trees discarded as burn-in. Each dataset was run twice to confirm repeatability. Results were analyzed using Tracer v.1.7, ensuring that the effective sample sizes (ESS) for all relevant parameters exceeded 200. Demographic reconstructions were plotted in R v.3.2.3 using the R script plot EBSP.R (Heled & Drummond, 2008).

RESULTS

Phylogenetic relationships

The ML and BI analyses, based on complete mitogenomes, yielded similar tree topologies. Bootstrap values indicated significant support for all nodes. *Naemorhedus* and *Capricornis* were monophyletic sister genera (Figure 2). Three major phylogenetic clades were identified within *Capricornis*: 1) *C. crispus*; 2) *C. swinhoei* and *C. rubidus*; and 3) *C. milneedwardsii*, *C. thar*, and *C. sumatraensis*. The five *Capricornis* sequences collected in this study clustered within the third branch, along with *C. milneedwardsii*, *C. thar*, and *C. sumatraensis*. Two major phylogenetic clades were identified within the *Naemorhedus*: 1) *N. cranbrooki*, *N. baileyi*, and *N. evansi*—with *N. cranbrooki* and *N. baileyi* forming monophyletic taxa; and 2) *N. griseus*, *N. goral*, and *N. caudatus*. In addition, *N. cranbrooki* was divided into two distinct subclades, with our *N. cranbrooki* sequences from Xizang clustering in one subclade and those from northern Myanmar clustering in another. Similarly, *N. evansi* was divided into two different subclades, with our sequences from Yunnan and northern Myanmar grouped together, and *N. baileyi* was divided into two different subclades. The *Muntiacus* species formed two major clades (Figure 2): 1) *M. reevesi*, *M. vuquangensis*, and *M. putaoensis*; and 2) *M. feae*, *M. gongshanensis*, *M. crinifrons*, red muntjac (*M. vaginalis*, *M. muntjak*, and *M. malabaricus*), and *M. atherodes*. Both *M. crinifrons* and *M. gongshanensis* were identified as monophyletic, with *M. gongshanensis* further divided into two subclades. The sequences of *M. gongshanensis* from northern Myanmar were dispersed across both subclades.

Divergence times

The evolutionary tree topologies for *Capricornis, Naemorhedus*, and *Muntiacus* species were consistent with the phylogenetic tree topologies (Figure 2), thus the two trees were combined into a single unified tree.

The split between *Muntiacus* species and *Elaphodus cephalophus* occurred at 7.82 Ma (95% HPD=7.27–8.39). The split between *Capricornis* and *Naemorhedus* species occurred at 5.19 Ma (95% HPD=4.66–5.74), with two major branches of *Naemorhedus* separating 4.83 Ma (95% HPD=4.33–5.34). *Muntiacus atherodes* split from the common ancestor of red muntjacs+*M. feae*+*M. gongshanensis*+*M. crinifrons* at 3.11 Ma (95% HPD=2.85–3.38), while *M. reevesi* split from the common ancestor of *M. vuquangensis*+*M. putaoensis* at 3.04 Ma (95% HPD=2.76–3.11) and *M. vuquangensis* split from *M. putaoensis* at 2.26 Ma (95% HPD=2.03–2.5). The red muntjacs split from the common ancestor of *M. feae*+*M. gongshanensis*+*M. crinifrons* at 2.69 Ma (95% HPD=2.46–2.92). *Capricornis crispus* diverged from the common ancestor of *Capricornis* species at 2.64 Ma (95% HPD=2.33–2.95). The split between *N. evansi* and the common ancestor of *N. cranbrooki* and *N. baileyi* occurred at 2.52 Ma (95% HPD=2.23–2.82). The common ancestor of *C. swinhoei* and *C. rubidus* diverged at 1.51 Ma (95% HPD=1.31–1.7), while the split between *N. cranbrooki* and *N. baileyi* occurred at 1.5 Ma (95% HPD=1.3–1.68). *Muntiacus feae* split with the common ancestor of *M. gongshanensis*+*M. crinifrons* at 1.24 Ma (95% HPD=1.1–1.37), while the split between *M. vaginalis* and *M. muntjak* occurred at 0.91 Ma (95% HPD=0.8–1.02).

Regarding the EHHM region, the split between *M. gongshanensis* and *M. crinifrons* occurred at 0.74 Ma (95% HPD=0.64–0.84), while the two subclades of *M. gongshanensis* split at 0.18 Ma (95% HPD=0.14–0.22). The mainland serow (*Capricornis sumatraensis*) predominantly divided into two main subclades at 0.42 Ma (95% HPD=0.36–0.48). The two subclades of *N. cranbrooki* split at 0.42 Ma (95% HPD=0.36–0.5), while the two subclades of *N. evansi* split at 0.35 Ma (95% HPD=0.29–0.42). A series of rapid divergences occurred within mainland serow between 0.38 Ma and 0.14 Ma.

Population dynamics

The EBSP analysis of *C. sumatraensis*, *N. cranbrooki*, *N. evansi*, and *M. gongshanensis* from the EHHM region is presented in Figure 3. The population of *C. sumatraensis* remained stable before 1.5 kilo annum (ka), after which it experienced an expansion. Similarly, the population of *N. cranbrooki* remained stable until approximately 1 Ma, followed by expansion. The populations of both *N. evansi* and *M. gongshanensis* were stable until approximately 8 ka, with population expansion occurring after that time.

DISCUSSION

Phylogenetic relationships, species differentiation, and refugia

Geological events, particularly the uplift of the Qinghai-Xizang Plateau, are considered key drivers of species divergence and population differentiation (Fu & Wen, 2023). The uplift of mountains creates physical barriers that promote species differentiation. The differentiation within *Capricornis*, *Naemorhedus*, and *Muntiacus* species is closely associated with multiple phases of uplift of the Qinghai-Xizang Plateau. The divergence between *Muntiacus* species and *E. cephalophus*, which occurred 7.82 Ma, may have been triggered by a slight uplift of Qinghai-Xizang Plateau at 8 Ma. The *Naemorhedus* and *Capricornis* species split around 5.19 Ma, with two major subclades of *Naemorhedus* diverging at approximately 4.83 Ma, corresponding to slight uplift of the Qinghai-Xizang Plateau and Hengduan Mountains. The

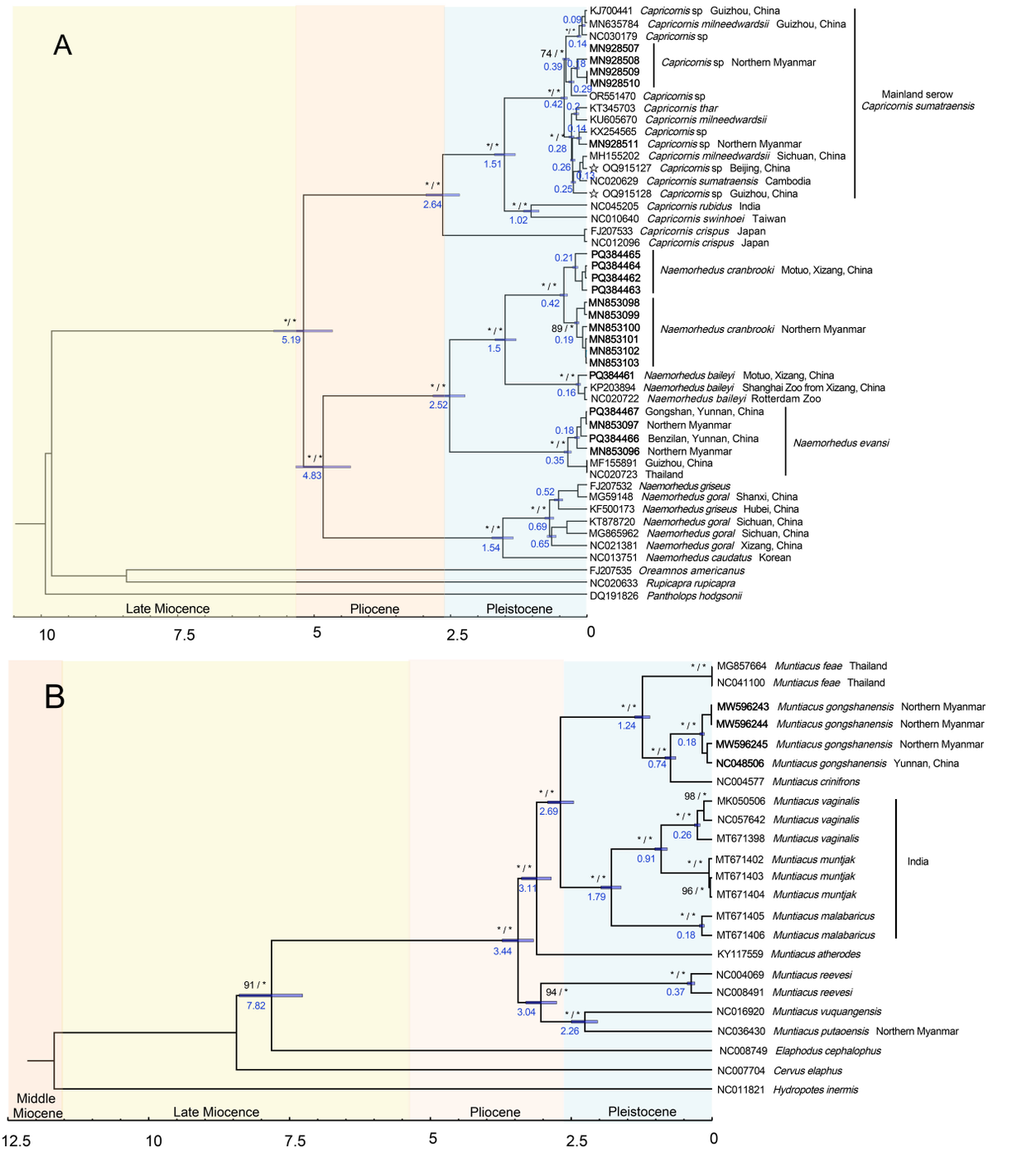

Figure 2 Unified maximum-likelihood (ML), Bayesian inference (BI) tree and estimation of divergence time based on complete mitogenomes

A: Unified tree of *Capricornis* and *Naemorhedus* species. B: Unified tree of *Muntiacus* species. Black numbers at nodes indicate maximum-likelihood and Bayesian posterior probability, respectively. Stars indicate values of 100 (ML) and 1.00 (BI). Blue numbers at nodes represent average time (Ma), blue bar represents 95% confidence interval. Sequences in bold are our samples. ☆ indicates sample is an ancient individual (sub-fossils).

geographic barriers formed by the A phase of the Qinghai-Xizang Movement may have contributed to the divergences of *M. atherodes* and *M. reevesi*, which occurred at 3.11 Ma and 3.04 Ma, respectively. The split between the three red muntjac species and the common ancestor of *M. feae*+*M. gongshanensis*+*M. crinifrons* occurred at 2.69 Ma, while the divergence between *N. evansi* and the common ancestor of *N. cranbrooki*+*N. baileyi* occurred around 2.52 Ma. Both of these events may have been triggered by mountain uplift during the B phase of the Qinghai-Xizang Movement. The basal species *C. crispus*, which inhabits the islands of Japan, diverged from the common ancestor of other serows around 2.64 Ma, coinciding with the appearance of the Tsushima Strait land bridge during the late Pliocene, which connected Japan and

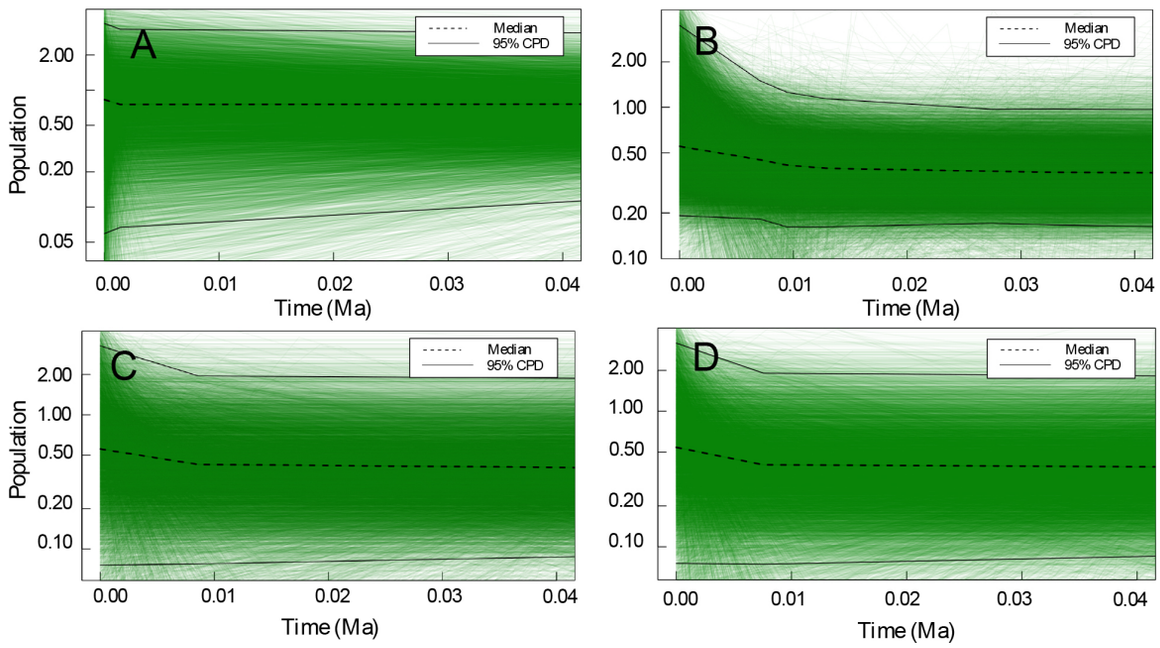

Figure 3 Extended Bayesian skyline plot (EBSP) analysis of *Capricornis sumatraensis*, *Naemorhedus cranbrooki*, *Naemorhedus evansi*, and *Muntiacus gongshanensis* in the East Himalaya-Hengduan Mountains based on complete mitogenomes

A: EBSP analysis of *C. sumatraensis*. B: EBSP analysis of *N. cranbrooki*. C: EBSP analysis of *N. evansi*. D: EBSP analysis of *M. gongshanensis*. X axis represents time in million of years (Ma). Y axis represents effective population size. Black dashed line represents median of population size, and green shaded area represents 95% Central Posterior Density (CPD).

Mainland of China (Kimura, 1977, 1996). After disappearance of the land bridge at 3 Ma, species may be isolatied (Kimura, 2002; Ogasawara, 1994). Additional divergences occurred between *C. sumatraensis* and the common ancestor of *C. swinhoei*+*C. rubidus* approximately around 1.51 Ma, between *N. cranbrooki* and *N. baileyi* around 1.5 Ma, and between *M. feae* and the common ancestor of *M. gongshanensis*+*M. crinifrons* approximately at 1.24 Ma. These divergences were likely driven by habitat fragmentation resulting from the C phase of the Qinghai-Xizang Movement.

Pleistocene glaciers may have isolated populations into refugia and promoted population differentiation and intra-specific diversification without apparent geological breaks (Hewitt, 2000). Our divergence analysis supported the interspecific and intraspecific differentiation of *Capricornis*, *Naemorhedus*, and *Muntiacus* species were closely linked to a series of Pleistocene glaciers. The divergence between *M. vaginalis* and *M. muntjak* occurred approximately 0.91 Ma, coinciding with the Xixiabangma glaciation (0.8–1.17 Ma; Zheng et al., 2002). This glaciation likely contributed to speciation, as arid regions of central India were unsuitable for many species, forcing populations to seek refuge in more favorable forested habitats in the northern and southern regions of the Indian subcontinent (Martins et al., 2017). The divergence between *M. gongshanensis* and *M. crinifrons*, two independent species, occurred around 0.74 Ma, likely due to the significant mountain uplift during the Kunlun-Huanghe Movement (1.1–0.7 Ma). The development of glaciers possibly forced these species to retreat to different refugia within the EHHM region. Subsequently, the distribution range of *M. crinifrons* likely expanded during the interglacial period. Consistent with the findings of Mori et al. (2019), our results showed that *C. thar*, *C. sumatraensis*, and *C. milneedwardsii* clustered into a single clade, but were not monophyletic, suggesting they may represent a single species (*C. sumatraensis*). The Naynayxungla glaciation, the most extensive glaciation event impacting the EHHM region (Wu et al., 2022; Zheng et al., 2002), likely contributed to the intraspecific differentiation of *C. sumatraensis* and *N. cranbrooki* around 0.42 Ma, and of *N. evansi* around 0.35 Ma (95% HPD=0.29–0.42). In the case of *C. sumatraensis*, the population was divided into two subclades, with samples from northern Myanmar dispersed across both clades. Similarly, *N. cranbrooki* samples from northern Myanmar and Xizang were divided into two subclades. We speculate that glacial expansion forced these populations into different refugia within the EHHM region, where they survived. A series of rapid intraspecific differentiations occurred in *C. sumatraensis* between 0.39 Ma and 0.07 Ma, potentially driven by the glacial and interglacial cycles, suggesting repeated dispersal occured centering from different refugia during the Quaternary period. According to Song et al. (2023), the regional extirpation of serows in northern China may have occurred without significant impact on genetic diversity, as individuals from Beijing and Baoxing (Sichuan) are closely related. A possible regional replacement in Guizhou, driven by maternal lineage, is indicated by sub-fossils from Guizhou and all modern serows from the same area clustering into different subclades. The intraspecific differentiation of *N. cranbrooki* was likely triggered by the Naynayxungla glaciation, which forced populations to retreat into refugia in Xizang and northern Myanmar. *Naemorhedus evansi* was divided into two subclades: One consisting of samples from Thailand and Guizhou (China), and the other from Myanmar and Yunnan (China). This divergence potentially occurred on both sides of the Nu-Salween River, which formed in the middle Neogene period (4.2–5.0 Ma) (Zhao et al., 2011). Glaciers and seasonal snowpacks, essential for regional water cycles, influence the flow of downstream water resources (Hugonnet et al., 2021; Zemp et al., 2019). Thus, we speculate that the Nu-Salween River may have experienced several low flow periods under the influence of the Xixia Bangma Glacier, similar to those of

the Yarlung Zangbo River (Wu et al., 2022), potentially enabling *N. evansi* to cross the river at shallow points. In addition, the valley glaciers formed during the glacial period may also have served as natural bridges for *N. evansi* dispersal. The intraspecific differentiation of *M. gongshanensis* around 0.18 Ma also suggests the presence of different refugia within the EHHM region during the Guxiang glacial period.

Species population expansion

The EBSP analyses revealed that the population expansions of *N. cranbrooki*, *N. evansi*, and *M. gongshanensis* in the EHHM region began between 10 and 8 ka, coinciding with the early to mid-Holocene period (11–7 ka). During this time, the Northern Hemisphere experienced rapid warming and increased humidity, primarily due to the retreat of continental ice sheets and orbital-induced changes in seasonal insolation (Zhang et al., 2022). These climatic shifts during the early Holocene promoted vegetation growth, particularly temperate deciduous broadleaf forests. In the middle Holocene (7–3 ka), although the climate became slightly drier, it still provided a relatively warm environment (Zhang et al., 2021a). Global warming likely had a pronounced effect on vegetation phenology in high-altitude mountain regions, extending the vegetative period (Kullman, 2004) and increasing food availability and energy for herbivores, thus facilitating population growth. Consequently, for herbivorous species inhabiting extreme mountain environments, where food availability is limited by cold temperatures during the growing season (Ciach & Pęksa, 2018), this climatic improvement likely had a positive effect on their survival and reproduction. Winter is a particularly critical period for offspring survival (Willisch et al., 2013), and the warmer winter climate of the Holocene, compared to the Pleistocene, would have been conducive to survival. As herbivorous ungulates adapted to high mountain regions, the population expansions of *N. cranbrooki*, *N. evansi*, and *M. gongshanensis* were highly consistent with the warmer Holocene climate. EBSP analysis indicated that the population expansion of *C. sumatraensis* in the EHHM region began approximately 1.5 ka, during the late Holocene. At that time, environmental conditions on the Qinghai-Xizang Plateau deteriorated, with lower temperatures and reduced precipitation leading to forest retreat toward the southeastern margin (Zheng & Li, 1999). This environmental shift may have driven the serow to migrate toward the southeastern regions, contributing to its population expansion in the EHHM. Furthermore, after 1.6 ka, intensified human settlement and grazing activities on the northeastern Qinghai-Xizang Plateau (Huang et al., 2017) may have further displaced *C. sumatraensis*, promoting its population expansion in the EHHM region.

The differentiation between *N. baileyi* and *N. cranbrooki* occurred approximately 1.5 Ma, then *N. cranbrooki* was divided into two different subclades: The Xizang population of China and the northern Myanmar population, with differentiation taking place during the Naynayxungla glaciation. Our research suggests that the *N. baileyi* and the *N. cranbrooki* should be recognized as two distinct species. Furthermore, intraspecific populations of *N. cranbrooki* have diverged into two geographic populations due to prolonged isolation, contrasting with previous findings and studies that *N. baileyi* and *N. cranbrooki* are homonyms (Groves & Grubb, 2011) and that *N. cranbrooki* is only distributed in northern Myanmar (Li et al., 2020). Our specimens from Xizang, China, support the distribution of *N. cranbrooki* within the coordinates of E96°to E98° longitude and N27°to N29°30' latitude (Hayman, 1961), encompassing the region of Xizang in China and northern Myanmar. Unfortunately, *N. cranbrooki* has not been recorded in China's Red List of Biodiversity: Vertebrates (Jiang et al., 2020) or Catalogue of mammals in China (Wei et al., 2021). Both *N. baileyi* and *N. cranbrooki* are red gorals, characterized by a warm brown to fox red coloration on most of their heads, bodies and limbs, along with a black dorsal stripe running from the nape to the base of the tail (Hayman, 1961; Groves & Grubb, 2011). The *N. cranbrooki* is darker in color and has a more pronounced stripe on its back. Compared with *N. cranbrooki*, *N. baileyi* has white patches on its pharynx and throat, while the *N. cranbrooki* does not. Based on molecular and morphological evidence, we believe that the *N. baileyi* and *N. cranbrooki* are two independent species. However, additional specimens from northern Myanmar need to be collected to determine whether *N. baileyi* is distributed in northern Myanmar and whether it arrived at different refugia (such as Xizang, China and northern Myanmar) during the glacial period, similar to *N. cranbrooki*. In addition, although the distribution range of the *N. evansi* was previously thought to extend from Thailand to central China (Li et al., 2020), the molecular evidence in Yunnan is lacking. For the first time, we collected one specimen each from Gongshan and Benzilan in Yunnan to address the gap in molecular evidence for *N. evansi* in this region.

It's worth noting that the sequence MH155202 of serow ought to be *C. milneedwardsii* which belongs to a subspecies of *C. sumatraensis* in the original documentary record (Zhao et al., 2019), but it is listed as *C. sumatraensis* in NCBI. Accurate species identification is crucial for subsequent studies, and we recommend that this sequence be correctly classified as *C. milneedwardsii* in NCBI to ensure taxonomic precision.

SCIENTIFIC FIELD SURVEY PERMISSION INFORMATION

Sample collections were conducted in Myanmar under permission number 1567/XTBG/2017, issued by the Forest Research Institute, Forest Department, Ministry of Environmental Conservation and Forestry of Myanmar, date 31 March. 2017.

DATA AVAILABILITY

Assembled mitochondrial genome sequences were deposited in the National Center for Biotechnology Information (NCBI) database (https://www.ncbi.nlm. nih.gov) under GenBank accession no. PQ384461–PQ384466 and Science Data Bank (https://doi.org/10.57760/sciencedb.11986).

SUPPLEMENTARY DATA

Supplementary data to this article can be found online.

COMPETING INTERESTS

The authors declare that they have no competing interests.

AUTHORS' CONTRIBUTIONS

G.G.L. conceived and supervised the project. G.G.L., Y.H.L., and N.S. prepared the samples and Y.X.M. performed bioinformatic analyses. P.Z.Y. helped with the bioinformatic analyses. Y.X.M. and G.G.L. preformed the experiments. Y.X.M. wrote the manuscript with input from all authors. Y.F. revised the manuscript. All authors read and approved the final version of the manuscript.

ACKNOWLEDGMENTS

This work was supported by the Forest Research Institute, Hponkanrazi Wildlife Sanctuary, and Hkakaborazi National Park Offices, Myanmar. Laboratory work was completed in the Central Laboratory, Public Technology Service Center, Xishuangbanna Tropical Botanical Garden (XTBG), CAS and the laboratory in the School of Life Sciences, Qinghai Normal University.

REFERENCES

Antonelli A, Nylander JAA, Persson C, et al. 2009. Tracing the impact of the Andean uplift on Neotropical plant evolution. *Proceedings of the National Academy of Sciences of the United States of America*, **106**(24): 9749–9754.

Barnosky AD. 2005. Effects of quaternary climatic change on speciation in mammals. *Journal of Mammalian Evolution*, **12**(1-2): 247–264.

Bartlein PJ, Colin Prentice I, Webb III T. 1986. Climatic response surfaces from pollen data for some Eastern North American Taxa. *Journal of Biogeography*, **13**(1): 35–57.

Beller HR, Chain PSG, Letain TE, et al. 2006. The genome sequence of the obligately chemolithoautotrophic, facultatively anaerobic bacterium *Thiobacillus denitrificans*. *Journal of Bacteriology*, **188**(4): 1473–1488.

Bibi F. 2013. A multi-calibrated mitochondrial phylogeny of extant Bovidae (Artiodactyla, Ruminantia) and the importance of the fossil record to systematics. *BMC Evolutionary Biology*, **13**: 166.

Bouckaert R, Heled J, Kühnert D, et al. 2014. BEAST 2: a software platform for Bayesian evolutionary analysis. *PLoS Computational Biology*, **10**(4): e1003537.

Burland TG. 2000. Dnastar's lasergene sequence analysis software. *In*: Misener S, Krawetz SA. Bioinformatics Methods and Protocols. Totowa: Humana Press, 71–91.

Cai MT, Fang XM, Wu FL, et al. 2012. Pliocene-Pleistocene stepwise drying of Central Asia: evidence from paleomagnetism and sporopollen record of the deep borehole SG-3 in the western Qaidam basin, NE Tibetan Plateau. *Global and Planetary Change*, **94–95**: 72–81.

Candy I. 2023. Understanding Quaternary climate change. *In*: Elias SA. Encyclopedia of Quaternary Science: Reference Module in Earth Systems and Environmental Sciences. Amsterdam: Elsevier.

Ciach M, Pęksa Ł. 2018. Impact of climate on the population dynamics of an alpine ungulate: a long-term study of the Tatra chamois *Rupicapra rupicapra tatrica*. *International Journal of Biometeorology*, **62**(12): 2173–2182.

Cui ZJ, Chen YX, Zhang W, et al. 2011. Research history, glacial chronology and origins of Quaternary glaciations in China. *Quaternary Sciences*, **31**(5): 749–764. (in Chinese)

Cui ZJ, Wu YQ, Liu GN, et al. 1998. On Kunlun-Yellow River tectonic movement. *Science in China Series D: Earth Sciences*, **41**(6): 592–600.

Domingo L, Koch PL, Hernández Fernández M, et al. 2013. Late Neogene and early Quaternary paleoenvironmental and paleoclimatic Conditions in Southwestern Europe: Isotopic analyses on mammalian taxa. *PLoS One*, **8**(5): e63739.

Dong W. 2007. New material of Muntiacinae (Artiodactyla, Mammalia) from the Late Miocene of the northeastern Qinghai-Tibetan Plateau, China. *Comptes Rendus Palevol*, **6**(5): 335–343.

Dou HL, Zhang YS, Feng LM. 2016. Complete mitochondrial genome of the Himalayan serow (*Capricornis thar*) and its phylogenetic status within the genus *Capricornis*. *Biochemical Systematics and Ecology*, **65**: 115–123.

Fjeldsaå J, Lovett JC. 1997. Biodiversity and environmental stability. *Biodiversity & Conservation*, **6**(3): 315–323.

Frenzel B, Bräuning A, Adamczyk S. 2003. On the problem of possible last-glacial forest-refuge-areas within the deep valleys of eastern Tibet. *Erdkunde*, **57**(3): 182–198.

Fu ZJ, Wen LY. 2023. Impacts of Quaternary glaciation, geological history and geography on animal species history in continental East Asia: a phylogeographic review. *Molecular Ecology*, **32**(16): 4497–4514.

Geissmann T, Lwin N, Aung SS, et al. 2011. A new species of snub-nosed monkey, genus *Rhinopithecus* Milne-Edwards, 1872 (primates, Colobinae), from northern Kachin State, northeastern Myanmar. *American Journal of Primatology*, **73**(1): 96–107.

Gibbard PL. 2015. The Quaternary System/Period and its major subdivisions. *Russian Geology and Geophysics*, **56**(4): 686–688.

Groves C, Grubb P. 2011. Ungulate Taxonomy. Baltimore: The Johns Hopkins University Press.

Groves CP, Grubb PJ. 1985. Reclassification of the Serows and Gorals (*Nemorhaedus*: Bovidae). London: Croom Helm Editions.

Gómez A, Lunt DH. 2007. Refugia within refugia: Patterns of phylogeographic concordance in the Iberian Peninsula. *In*: Weiss S, Ferrand N. Phylogeography of Southern European Refugia. Dordrecht: Springer, 155–188.

Hassanin A, Delsuc F, Ropiquet A, et al. 2012. Pattern and timing of diversification of Cetartiodactyla (Mammalia, Laurasiatheria), as revealed by a comprehensive analysis of mitochondrial genomes. *Comptes Rendus Biologies*, **335**(1): 32–50.

Hayman RW. 1961. The red goral of the north-east frontier region. *Journal of Zoology*, **136**(3): 317–323.

Head MJ, Gibbard PL. 2015. Formal subdivision of the Quaternary System/Period: past, present, and future. *Quaternary International*, **383**: 4–35.

Heled J, Drummond AJ. 2008. Bayesian inference of population size history from multiple loci. *BMC Evolutionary Biology*, **8**: 289.

Hewitt G. 2000. The genetic legacy of the Quaternary ice ages. *Nature*, **405**(6789): 907–913.

Higgins DG, Sharp PM. 1988. CLUSTAL: a package for performing multiple sequence alignment on a microcomputer. *Gene*, **73**(1): 237–244.

Hu QM. 1994. On the geographical distribution of the Primulaceae. *Journal of Tropical and Subtropical Botany*, **2**(4): 1–14.

Huang XZ, Liu SS, Dong GH, et al. 2017. Early human impacts on vegetation on the northeastern Qinghai-Tibetan Plateau during the middle to late Holocene. *Progress in Physical Geography: Earth and Environment*, **41**(3): 286–301.

Hugonnet R, McNabb R, Berthier E, et al. 2021. Accelerated global glacier mass loss in the early twenty-first century. *Nature*, **592**(7856): 726–731.

Jia DR, Abbott RJ, Liu TL, et al. 2012. Out of the Qinghai-Tibet plateau: Evidence for the origin and dispersal of Eurasian temperate plants from a phylogeographic study of *Hippophaë rhamnoides* (Elaeagnaceae). *New Phytologist*, **194**(4): 1123–1133.

Jiang ZG, Wu Y, Liu SY, et al. 2020. China's Red List of Biodiversity: Vertebrates, Volume I, Mammals.

Kalyaanamoorthy S, Minh BQ, Wong TKF, et al. 2017. ModelFinder: fast model selection for accurate phylogenetic estimates. *Nature Methods*, **14**(6): 587–589.

Kimura M. 1977. Palaeogeography of the Ryukyu Arc. *Chikyu Monthly*.

Kimura M. 1996. Quaternary paleogeography of the Ryukyu Arc. *Journal of Geography* (*Chigaku Zasshi*), **105**(3): 259–285.

Kimura M. 2002. The Formation of the Ryukyu Arc and Migration of Biota to the Arc. Naha: Okinawa Times.

Kullman L. 2004. Long-term geobotanical observations of climate change impacts in the Scandes of west-Central Sweden. *Nordic Journal of Botany*, **24**(4): 445–467.

Li GG, Sun N, Swa K, et al. 2020. Phylogenetic reassessment of gorals with new evidence from Northern Myanmar reveals five distinct species. *Mammal Review*, **50**(4): 325–330.

Li GG, Zhang MX, Swa K, et al. 2017. Complete mitochondrial genome of the leaf muntjac (*Muntiacus putaoensis*) and phylogenetics of the genus

Muntiacus. *Zoological Research*, **38**(5): 310–316.
Li JJ, Fang XM, Pan BT, et al. 2001. Late Cenozoic intensive uplift of Qinghai-Xizang Plateau and its impacts on environments in surrounding area. *Quaternary Sciences*, **21**(5): 381–391. (in Chinese)
Li JJ, Shu Q, Zhou SZ, et al. 2004. Review and prospects of Quaternary glaciation research in China. *Journal of Glaciology and Geocryology*, **26**(3): 235–243. (in Chinese)
Li JJ, Zhou SZ, Zhao ZJ, et al. 2015. The Qingzang movement: the major uplift of the Qinghai-Tibetan plateau. *Science China Earth Sciences*, **58**(11): 2113–2122.
Liow LH, Fortelius M, Bingham E, et al. 2008. Higher origination and extinction rates in larger mammals. *Proceedings of the National Academy of Sciences of the United States of America*, **105**(16): 6097–6102.
Liu YB, Jiang LC. 2017. The complete mitochondrial genome sequence of the Himalayan goral, *Naemorhedus goral* (Cetartiodactyla: Caprinae). *Mitochondrial DNA Part A*, **28**(2): 233–235.
Lorenzen ED, Nogués-Bravo D, Orlando L, et al. 2011. Species-specific responses of Late Quaternary megafauna to climate and humans. *Nature*, **479**(7373): 359–364.
Lwin YH, Wang L, Li GG, et al. 2021. Diversity, distribution and conservation of large mammals in northern Myanmar. *Global Ecology and Conservation*, **29**: e01736.
Ma YZ, Liu KB, Feng ZD, et al. 2013. Vegetation changes and associated climate variations during the past ~38, 000 years reconstructed from the Shaamar eolian-paleosol section, northern Mongolia. *Quaternary International*, **311**: 25–35.
Mapelli FJ, Mora MS, Mirol PM, et al. 2012. Effects of Quaternary climatic changes on the phylogeography and historical demography of the subterranean rodent *Ctenomys porteousi*. *Journal of Zoology*, **286**(1): 48–57.
Martins RF, Fickel J, Le M, et al. 2017. Phylogeography of red muntjacs reveals three distinct mitochondrial lineages. *BMC Evolutionary Biology*, **17**(1): 34.
Mead JI. 1989. *Nemorhaedus goral*. *Mammalian Species*, **335**: 1–5.
Meng LH, Chen G, Li ZH, et al. 2015. Refugial isolation and range expansions drive the genetic structure of *Oxyria sinensis* (Polygonaceae) in the Himalaya-Hengduan Mountains. *Scientific Reports*, **5**: 10396.
Miller EF, Manica A, Amos W. 2018. Global demographic history of human populations inferred from whole mitochondrial genomes. *Royal Society Open Science*, **5**(8): 180543.
Morales-Barbero J, Martinez PA, Ferrer-Castán D, et al. 2018. Quaternary refugia are associated with higher speciation rates in mammalian faunas of the Western Palaearctic. *Ecography*, **41**(4): 607–621.
Mori E, Nerva L, Lovari S. 2019. Reclassification of the serows and gorals: the end of a neverending story?. *Mammal Review*, **49**(3): 256–262.
Myers N, Mittermeier RA, Mittermeier CG, et al. 2000. Biodiversity hotspots for conservation priorities. *Nature*, **403**(6772): 853–858.
Ogasawara K. 1994. Neogene paleogeography and marine climate of the Japanese Islands based on shallow-marine molluscs. *Palaeogeography, Palaeoclimatology, Palaeoecology*, **108**(3-4): 335–351.
Pang H, Liu W, Chen YG, et al. 2008. Identification of complete mitochondrial genome of the tufted deer. *DNA Sequence*, **19**(4): 411–417.
Petronio C, Krakhmalnaya T, Bellucci L, et al. 2007. Remarks on some Eurasian pliocervines: characteristics, evolution, and relationships with the tribe Cervini. *Geobios*, **40**(1): 113–130.
Rambaut A, Drummond AJ, Xie D, et al. 2018. Posterior summarization in Bayesian phylogenetics using Tracer 1.7. *Systematic Biology*, **67**(5): 901–904.
Raymo ME, Ruddiman WF. 1992. Tectonic forcing of Late Cenozoic climate. *Nature*, **359**(6391): 117–122.
Rozewicki J, Li SL, Mar AK, et al. 2019. MAFFT-DASH: integrated protein sequence and structural alignment. *Nucleic Acids Research*, **47**(W1): W5–W10.
Schaefer JM, Finkel RC, Balco G, et al. 2016. Greenland was nearly ice-free for extended periods during the Pleistocene. *Nature*, **540**(7632): 252–255.
Schmitt T, Varga Z. 2012. Extra-Mediterranean refugia: the rule and not the exception?. *Frontiers in Zoology*, **9**(1): 22.
Shi YF. 2002. Characteristics of late Quaternary monsoonal glaciation on the Tibetan Plateau and in East Asia. *Quaternary International*, **97–98**: 79–91.
Shi YF, Zheng BX, Li SJ. 1992. Last glaciation and maximum glaciation in the Qinghai-Xizang (Tibet) Plateau: a controversy to M. Kuhle's Ice Sheet Hypothesis. *Chinese Geographical Science*, **2**(4): 293–311.
Singh B, Kumar A, Uniyal VP, et al. 2021. Phylogeography and population genetic structure of red Muntjacs: evidence of enigmatic Himalayan red Muntjac from India. *BMC Ecology and Evolution*, **21**(1): 49.
Sinha A, Datta A, Madhusudan MD, et al. 2005. *Macaca munzala*: a new species from western Arunachal Pradesh, Northeastern India. *International Journal of Primatology*, **26**(4): 977–989.
Song SW, Xiao B, Hu JM, et al. 2023. Ancient mitogenomes reveal stable genetic continuity of the Holocene Serows. *Genes*, **14**(6): 1187.
Stewart JR, Lister AM, Barnes I, et al. 2010. Refugia revisited: individualistic responses of species in space and time. *Proceedings of the Royal Society B: Biological Sciences*, **277**(1682): 661–671.
Timmins R, Duckworth JW. 2016. *Muntiacus gongshanensis*. The IUCN red list of threatened species, e. T13926A22160596.
Velho N, Karanth KK, Laurance WF. 2012. Hunting: a serious and understudied threat in India, a globally significant conservation region. *Biological Conservation*, **148**(1): 210–215.
Wei FW, Yang QS, Wu Y, et al. 2021. Catalogue of mammals in China (2021). *Acta Theriologica Sinica*, **41**(5): 487–501.
Whittington-Jones GM, Bernard RTF, Parker DM. 2008. Bushclumps as refugia for small mammals in two eastern cape conservation areas. *African Zoology*, **43**(2): 273–276.
Willisch CS, Bieri K, Struch M, et al. 2013. Climate effects on demographic parameters in an unhunted population of alpine chamois (*Rupicapra rupicapra*). *Journal of Mammalogy*, **94**(1): 173–182.
Willner W, di Pietro R, Bergmeier E. 2009. Phytogeographical evidence for post-glacial dispersal limitation of European beech forest species. *Ecography*, **32**(6): 1011–1018.
Wu YN, Long D, Lall U, et al. 2022. Reconstructed eight-century streamflow in the Tibetan Plateau reveals contrasting regional variability and strong nonstationarity. *Nature Communications*, **13**(1): 6416.
Wu ZY. 1988. Hengduan mountain flora and her significance. *Journal of Japanese Botany*, **63**(9): 297–311.
Xu TT, Abbott RJ, Milne RI, et al. 2010. Phylogeography and allopatric divergence of cypress species (*Cupressus* L.) in the Qinghai-Tibetan Plateau and adjacent regions. *BMC Evolutionary Biology*, **10**: 194.
Yang FS, Li YF, Ding X, et al. 2008. Extensive population expansion of *Pedicularis longiflora* (Orobanchaceae) on the Qinghai-Tibetan plateau and its correlation with the quaternary climate change. *Molecular Ecology*, **17**(23): 5135–5145.
Yang Y, Youlatos D, Behie AM, et al. 2022. Positional behavior and canopy use of black snub-nosed monkeys *Rhinopithecus strykeri* in the Gaoligong Mountains, Yunnan, China. *Current Zoology*, **68**(4): 401–409.
Zachos J, Pagani M, Sloan L, et al. 2001. Trends, rhythms, and aberrations in global climate 65 Ma to present. *Science*, **292**(5517): 686–693.
Zemp M, Huss M, Thibert E, et al. 2019. Global glacier mass changes and their contributions to sea-level rise from 1961 to 2016. *Nature*, **568**(7752): 382–386.
Zhang CZ, Sheng HL, Lu HJ. 1984. On the Fea's Muntjak from Xijang

(Tibet). *Acta Theriolgica Sinica*, **2**: 88–106.

Zhang D, Gao FL, Jakovlić I, et al. 2020. PhyloSuite: an integrated and scalable desktop platform for streamlined molecular sequence data management and evolutionary phylogenetics studies. *Molecular Ecology Resources*, **20**(1): 348–355.

Zhang PZ, Zheng DW, Yin GM, et al. 2006. Discussion on late Cenozoic growth and rise of northeastern margin of the Tibetan Plateau. *Quaternary Sciences*, **26**(1): 5–13. (in Chinese)

Zhang WC, Wu HB, Cheng J, et al. 2022. Holocene seasonal temperature evolution and spatial variability over the Northern Hemisphere landmass. *Nature Communications*, **13**(1): 5334.

Zhang Y, Cui QY, Huang YL, et al. 2021a. Vegetation response to Holocene climate change in the Qinling mountains in the temperate-subtropical transition zone of central-east China. *Frontiers in Ecology and Evolution*, **9**: 734011.

Zhang YC, Lwin YH, Li R, et al. 2021b. Molecular phylogeny of the genus *Muntiacus* with special emphasis on the phylogenetic position of *Muntiacus gongshanensis*. *Zoological Research*, **42**(2): 212–216.

Zhao P, Xu HL, Li DY, et al. 2019. The complete mitochondrial genome sequence and phylogenetic analysis of Chinese Serow (*Capricornis Milneedwardsii*). *Mitochondrial DNA Part B*, **4**(1): 1922–1923.

Zhao XT, Wu ZH, Ye PS, et al. 2011. Discovery of neogene gravels and dammed-lake sediments in Nujiang (Salween) river valleys, Yunnan province, China, and their implications. *Acta Geologica Sinica*, **85**(12): 1963–1976. (in Chinese)

Zheng BX, Shi YF. 1976. Discussion Quaternary glaciation of mount Qomolangma area. *In*: Xizang Scientific Expedition of Chinese Academy of Sciencesed. Report of Qomolangma Area Scientific Expedition (1966–1968) Quaternary Geology. Beijing: Science Press, 29–62. (in Chinese)

Zheng BX, Xu QQ, Shen YP. 2002. The relationship between climate change and Quaternary glacial cycles on the Qinghai-Tibetan Plateau: review and speculation. *Quaternary International*, **97**–**98**: 93–101.

Zheng D, Li BY. 1999. Progress in studies on geographical environments of the Qianghai-Xizang plateau. *Scientia Geographica Sinica*, **19**(4): 295–302. (in Chinese)

Zu KL, Wang ZH. 2022. Research progress on the elevational distribution of mountain species in response to climate change. *Biodiversity Science*, **30**(5): 21451. (in Chinese)